Received: 16 February 2022 | Revised: 9 May 2022 | Accepted: 11 May 2022

DOI: 10.1002/pro.4356

FULL-LENGTH PAPER

3,4-Dihydroxyphenylethanol and 3,4-dihydroxyphenylacetic acid affect the aggregation process of E46K variant of α-synuclein at different extent: Insights into the interplay between protein dynamics and catechol effect

Benedetta Fongaro | Elia Cappelletto | Alice Sosic | Barbara Spolaore | Patrizia de Polverino de Laureto

Department of Pharmaceutical and Pharmacological Sciences, University of Padova, Padova, Italy

Correspondence
Patrizia Polverino de Laureto, Department of Pharmaceutical and Pharmacological Sciences, University of Padova, Padova, Italy.
Email: patrizia.polverinodelaureto@unipd.it

Funding information
Ministero dell'Istruzione, dell'Università e della Ricerca-PNRA, Grant/Award Number: PNRA18_00147; Progetti di Ateneo-University of Padova 2018, Grant/Award Number: SPOL_SID18_01; Progetti di Ateneo-University of Padova 2017 POLV_SID17 N, Grant/Award Number: C93C1800002600

Review Editor: Aitziber Cortajarena

Abstract

Parkinson's disease (PD) is a chronic multifactorial disease, whose etiology is not completely understood. The amyloid aggregation of α-synuclein (Syn) is considered a major cause in the development of the disease. The presence of genetic mutations can boost the aggregation of the protein and the likelihood to develop PD. These mutations can lead to early onset (A30P, E46K, and A53T) or late-onset (H50Q) forms of PD. The disease is also linked to an increase in oxidative stress and altered levels of dopamine metabolites. The molecular interaction of these molecules with Syn has been previously studied, while their effect on the pathological mutant structure and function is not completely clarified. By using biochemical and biophysical approaches, here we have studied the interaction of the familial variant E46K with two dopamine-derived catechols, 3,4-dihydroxyphenylacetic acid and 3,4-dihydroxyphenylethanol. We show that the presence of these catechols causes a decrease in the formation of amyloid fibrils in a dose-dependent manner. Native- and Hydrogen/deuterium exchange-mass spectrometry (HDX-MS) provide evidence that this effect is strongly conformation dependent. Indeed, these molecules interact differently with the interconverting conformers of Syn and its familial variant E46K in solution, selecting the most prone-to-aggregation one, confining it into an off-pathway oligomer. These findings suggest that catechols could be a molecular scaffold for the design of compounds potentially useful in the treatment of Parkinson's disease and related conditions.

KEYWORDS

DOPAC, DOPET, native and HDX-mass spectrometry, Parkinson disease, protein dynamics, α-synuclein

1 | INTRODUCTION

Parkinson disease (PD) is a multifactorial progressive neurodegenerative disorder, characterized mainly by motor symptoms, due to the selective death of dopaminergic neurons in the substantia nigra of the brain.[1] The majority of the PD cases are idiopathic, age dependent, while rare forms of autosomal dominant PD have been correlated with point mutations in α-synuclein (Syn). This protein, in its amyloid conformation, is one of the constituents of the filamentous cytoplasmic inclusions, called Lewy bodies, pathological hallmarks of PD.[2] The monomeric Syn is a natively unfolded protein in solution,[3] but it can adopt different conformations according to the cellular environment and the molecular interactions.[4] Membrane, lipids, and detergent induce Syn to acquire regular α-helical secondary structure[5–7] as well as affect the rate of Syn fibril formation.[8,9] In vitro and vivo, in its aggregated form, Syn conformation acquires β-sheet secondary structure and this process is closely associated with PD progression.[10] Three distinct structural domains conventionally form the Syn primary structure (Figure 1a). The N-terminal lipid-binding domain spans from residues 1 to 60 and contains seven imperfect 11-mer repeats (with the consensus XKTKEGVXXXX). The central domain (61–95) is called non-amyloid β-component (NAC) and is responsible for the amyloid properties of the protein. The C-terminal acidic tail is the target of posttranslational modifications and modulates the conversion of the protein in fibrils.[11,12]

The several recently discovered point mutations were found in the N-terminal region and can lead to early- (A30P, E46K, and A53T) or late- (H50Q) onset forms of PD.[13–16]

The consequences of these mutations on the structural and biological properties, on amyloid aggregation kinetics and on the affinity for lipid membrane of Syn were intensively studied. Wide evidence demonstrated that some familial variants (A53T, E46K, and H50Q) accelerate the aggregation process compared with the wild-type protein. Debated is the effect of the A30P mutation that seems to depend on the general experimental conditions, while the H50Q variant has been reported to aggregate more slowly than Syn.[17] Among the several variants, E46K mutation is shown to cause a severe clinical phenotype and to increase the toxicity of aggregated forms of Syn.[15,18] It was isolated from a Spanish family[15] and is generated by a single base pair change at position 188 in the exon 3 of Park1 gene locus. This mutation generates the little change in the molecular weight of Syn (0.9 Da difference) but inserts in the N-terminal region an extra positive charge. Its specific position in the sequence and its chemical nature together with the clinical profile manifested by patients suffering for this PD form closer to Lewy body dementia suggest that this variant might have a very critical and unique effect on the protein structure. Even though E46K seems to not affect the Syn physiological function in SNARE-complex assembly,[19] the large oligomers produced by this variant appear more toxic than those from the wild-type protein in a rat model of synucleinopathies[20] and E46K fibrils impair the mitochondrial activity at lower concentration than Syn.[21] Structurally the presence of the extra lysine residue determines several important consequences like an increase of the long-range intramolecular interactions between the C-terminal and the N-terminal regions of Syn.[22] The overall effect is a more compact structure in E46K mutant in respect of the wild-type protein.[23,24] The cryo-EM model of the N-terminal acetylated E46K fibrils reveals some differences with the fibrils formed by the wild-type protein. They appear less resistant to harsh conditions, proteolysis, prone to being fragmented with an enhanced seeding capability.[25] However, Boyer et al.[21] highlighted an important difference between E46K and wild-type fibril structures deriving from their pattern of electrostatic interactions (especially for the absence of E46-K80 salt bridge) that confer higher buried surface area to E46K fibrils, which present only a type of polymorph. In relation to the ability of Syn to interact with lipid interfaces, the extra K in the lipid binding domain affects membrane curvature selectivity,[26] the kinetics of membrane-induced amyloid formation[17] and a significant difference in the rate of association–dissociation on lipid surface, especially in the case of the E46K variant respect the wild-type protein.[27] The region acting as an

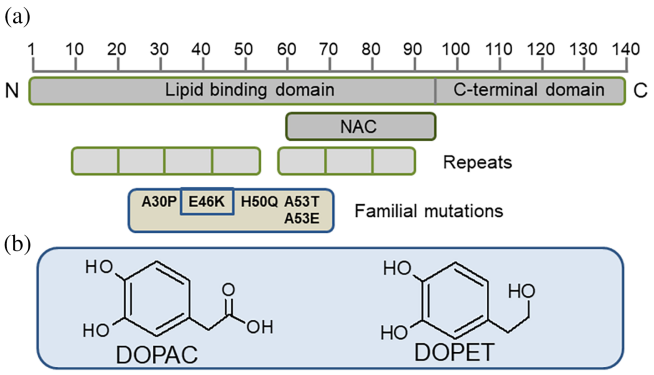

FIGURE 1 Sequence and structural domain organization of α-synuclein (a). The N-, C- and NAC regions are shown; the position of the mutations responsible for familial form of Parkinson's disease (PD) is indicated and the mutation E46K is highlighted. Residues 1–95 form the lipid-binding domain. Structures of 3,4-dihydroxyphenylacetic acid (DOPAC) and 3,4-dihydroxyphenylethanol (DOPET) (b)

anchor to lipid surface seems to extend up to residue 42, indicating a preference for the mutant for populating the membrane-bound state.[28]

Several strategies were proposed for prevention of Syn toxicity and to combat PD, targeting Syn. In consideration of the structural difference between Syn and its variants, it is not clear if the same treatment could be effective toward the pathology induced by Syn or by mutants. We are sighting to find molecules able to inhibit Syn fibril formation or to propose scaffolds for the synthesis of new drugs. Recently, we showed that 3,4-dihydroxyphenylacetic acid (DOPAC) and 3,4-dihydroxyphenylethanol (DOPET) hamper Syn from forming fibrils. These molecules are produced in vivo by dopamine metabolism and removed from the cells by active transport.[29] Their level was found altered by processes related to the onset of PD.[30,31] They are constituted by an aromatic ring bearing a substituent in position 5 that is an acetic acid side chain derived from aldehyde oxidation in DOPAC or an alcoholic moiety in DOPET. They undergo spontaneous oxidation to quinone derivatives, leading to the production of hydrogen peroxide providing in vivo increased oxidative stress.[32] DOPET is one of the major olive oil phenolic compounds and a derivative of Oleuropein aglycone (OleA) contained in olive leaves; therefore, its antiatherogenic, cardioprotective, anticancer, neuroprotective, and endocrine properties were correlated with the olive oil consumption.[33] DOPET shows antioxidant abilities, attributed to the presence of the *o*-dihydroxyphenyl moiety. Moreover, it stimulates the synthesis of antioxidant enzymes such as the activation of nuclear factor (erythroid-derived-2)-like 2 (Nrf2) and glutamate cysteine ligase modifier (GCLM).[34] We have shown that these catechols interact with Syn by covalent and noncovalent bonds, and the last ones play a key role in the fibril formation inhibition, inducing a significant modification in the relative proportion between soluble and insoluble, monomeric and oligomeric Syn. Catechol-induced protein species may be described as a protected and shielded population, whose structure is responsible for their overall biological and biophysical effects. Furthermore, catechols reduce the ROS produced by Syn aggregates that exhibited reduced interaction with cell membranes.[35–37]

Here, we have extended the study of these molecules in relation to the effects on the pathogenic mutant of Syn E46K. Several detailed reports of structure–function relation have demonstrated that the E46K mutation amplifies the neurotoxicity of Syn and consistently increases the rate at which Syn forms fibrils.[18,23] We used a biophysical approach capable of capturing the dynamic nature of these proteins in their native state. The intrinsic property of these proteins of being unfolded and to appear as an ensemble of energetically similar conformations complicates the rational design of targeted drugs. In fact, it has not been clarified which conformer present in the Syn population is the one most prone to forming fibrils and, therefore, potentially more toxic or possibly responsible for the onset of PD. Several catechol/protein ratios have been tested to show a dose-dependent effect and to highlight the difference between E46K and the wild-type protein in being affected by catechol in terms of aggregation inhibition and conformational preferences. By using native and HDX mass spectrometry techniques, we provided an insight into the molecular interplay between DOPAC and DOPET and the Syn variant E46K. We demonstrated that the different extent of aggregation inhibition induced by catechols was related to the different amounts of protein extended conformers versus the compact ones present at the equilibrium in the native state.

2 | RESULTS

2.1 | DOPAC and DOPET hamper E46K and Syn aggregation at different extent

E46K was left to aggregate in the absence and in the presence of DOPAC and DOPET by using different ratio protein/catechol (1:1, 1:2, and 1:5). To avoid the methionine oxidation and to exclude this parameter in the evaluation of the effects of catechols on the aggregation properties of E46K, catalase was added to the aggregation mixture. The experiments were conducted comparing side by side the results with those obtained with the wild-type protein (see also references 36,37). Different times of incubation have been tested (0, 48, 72, and 192 hr) corresponding to lag phase, elongation phase, and stationary phase in the fibril formation process. According to Greenbaum et al.[18] and Fredenburg et al.,[23] E46K and Syn exhibited different kinetics of fibril formation and the pathological variant aggregated most readily than the wild type, with a shorter lag time (Figures 2a and S1A). Figure 2a shows the effect of the two catechols on the protein aggregation probed by ThT fluorescence. By using a protein/catechol ratio of 1:1, partial inhibition of the aggregation propensity was observed for both molecules. However, it is evident that DOPAC appears more efficient than DOPET at this ratio and E46K is less sensitive to the catechol. At higher ratios, the formation of fibrils appeared substantially (for the 1:2 ratio) or completely (for the 1:5 ratio) inhibited. Plotting the inhibition response as a function of the catechol concentration (Figures 2 and S1B), evidence of a dose-dependent effect of catechols is clearly provided. To determine the secondary structure changes of E46K associated with the protein aggregation, CD in the far UV

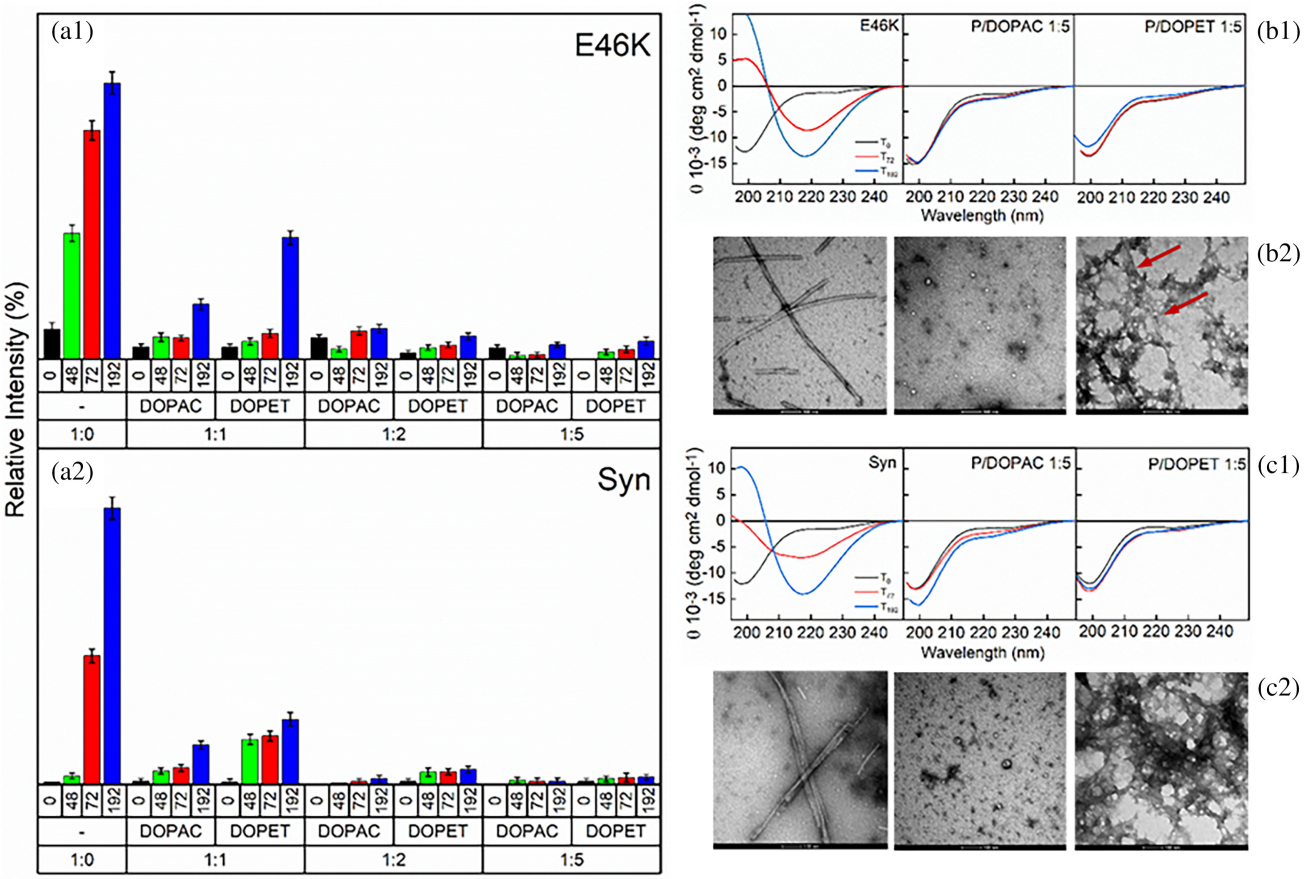

FIGURE 2 Aggregation process of E46K and Syn, in the absence (1:0) and in the presence of 3,4-dihydroxyphenylacetic acid (DOPAC) and 3,4-dihydroxyphenylethanol (DOPET) different molar ratio (1:1, 1:2, 1:5) probed by ThT assay (a). Aliquots were taken at the time points 0 (black), 48 (green), 72 (red) and 192 (blue) hr from the aggregation mixtures corresponding to steps containing oligomers (48–72 hr) and fibrils (192 hr). Far-UV CD spectra of E46K (b_1) and Syn (c_1). Spectra of each protein were obtained after 0, 72, and 192 hr of incubation under shaking at 37°C, in the absence and in the presence of DOPAC and DOPET at the reported ratio. Measurements were recorded in 20 mM sodium phosphate buffer, at 0.1 mg/ml protein concentration. TEM images of protein material corresponding to samples of E46K (b_2) and Syn (c_2) incubated for ~190 hr in the absence of the catechol (left), in the presence of DOPAC (center), and in the presence of DOPET (right). The images were obtained with an enlargement of 100 nm. The red arrows indicate fibrils still present in the sample.

measurements were performed (Figure 2b_1). In the absence of DOPAC and DOPET, the protein adopted predominantly β-sheet structure after incubation according to the fibril formation. Conducting the experiments in the presence of catechols, the protein CD spectra recorded on samples collected after 72 and 192 hr of incubation indicated predominantly a random coil conformation and the spectra appeared superimposable to those of the monomeric protein recorded at the beginning of the aggregation and in the absence of catechols. In Figure 2c_1, the same measurements were reported for Syn for comparison.

The morphology of the fibrils of Syn strongly depends on different assembly conditions, and such polymorphism reflects the ability of soluble protein to populate multiple conformational states before aggregation.[21,38] Under the conditions used in the present work, the fibrils formed by E46K exhibited a slightly different morphology from that of the fibrils generated by Syn, as assessed by TEM (Figure 2b_2,c_2). They appeared unbranched with a diameter of ~11–14 nm, while fibrils generated by Syn presented a smaller diameter of ~8.0–10 nm (see also references 35,36). Moreover, E46K fibrils resulted to be broken (even if samples were not frozen) and organized as a single fibril, differently from Syn, in which fibrils are intact and composed of a bundle structure, suggesting a different fibril structure. The interaction with the catechols led to the formation of structures different from fibrils, which were readily identified as off-pathway aggregates. The presence of DOPAC (1:5) (Figure 2b_2,c_2, middle pictures) induced the generation of spherical and annular species, which appeared slightly smaller in the case of E46K (~10–20 nm) in respect of those formed by Syn (~20–40 nm). The incubation of the proteins with

DOPET (right picture) led to the growth of amorphous structures, characterized by a scarce population of well-defined oligomers. In the samples of E46K/DOPET, fibrils were still detectable, consistently with the lower efficacy of DOPET than DOPAC in the aggregation inhibition.

2.2 | E46K extensively oligomerizes in the presence of catechols

It was previously found that Syn, incubated in the presence of catechols, gave rise to off-pathway oligomers, mainly dimers and trimers and these species are chemically modified for the formation of adducts due to the covalent reaction of either DOPAC or DOPET quinone with the side chains of Lys residues.[36,37] These two aspects were evaluated for E46K by size exclusion chromatography (SEC) and RP-HPLC comparing the chromatograms of samples taken from the aggregation mixture in correspondence of time points where the mutant is expected to populate mainly transient oligomers or fibrils with those obtained for Syn. The large and insoluble aggregates were removed by centrifugation before loading the samples onto the SEC column. At the beginning of the incubation, E46K alone showed a main peak at 15 ml elution volume corresponding to a value of MW in the calibration curve compatible with the monomeric protein (Figure 3a, inset, M). Upon incubation, the protein undergoes aggregation and the intensity of this peak largely decreased due to fibril growth. When protein/catechol samples were investigated, new additional peaks corresponding to trimer (T, 11.1 ml) and dimer (D, 12.3 ml) were detected before the monomeric species (M) (Figure 3a; T and D). In addition, in this range of elution volumes, the baseline increasingly shifted upwards proportionally to the molar concentration of catechol. These findings indicated that, in the presence of DOPAC and DOPET, E46K gave rise to several aggregated species that were not present when the protein is incubated alone; these species eluted before the monomeric protein, thus indicating their greater hydrodynamic volume. The drop-in intensity of the monomeric peak after incubation is due to insoluble fibrils formation in the case of the protein alone and to the formation of other soluble aggregates in the presence of DOPAC or DOPET. Considering that the main peak eluted in the presence of DOPAC and DOPET contained the protein modified by the catechol, this species was indicated as M* to distinguish it from the monomer containing only the protein. The area of the peaks relative to the dimer (D) and the trimer (T) forms from SEC was plotted as a function of the incubation time both in the absence and in the presence of catechols to quantify the level of oligomerization induced by the

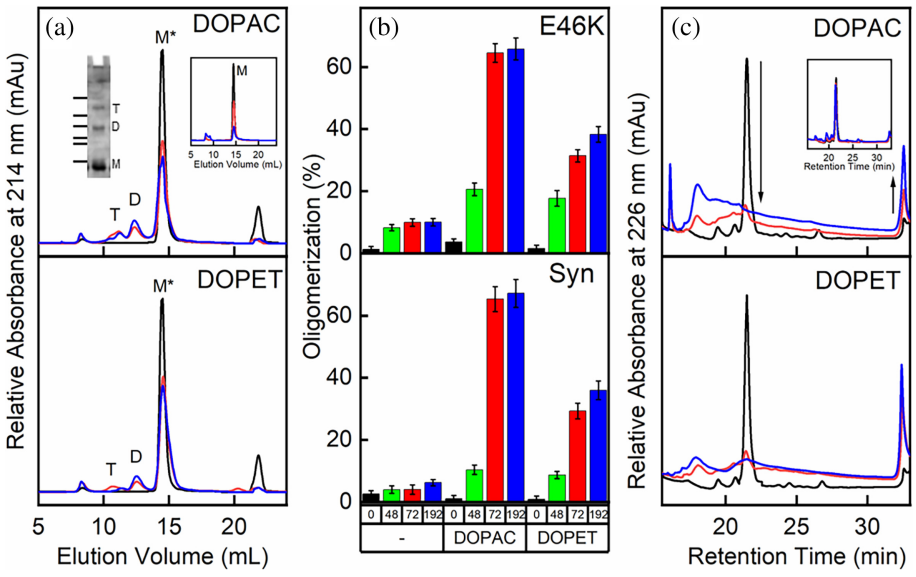

FIGURE 3 Aggregation process of E46K in the absence (insert) and in the presence of 3,4-dihydroxyphenylacetic acid (DOPAC) and 3,4-dihydroxyphenylethanol (DOPET) (protein/catechol 1:5) assessed by SEC (a) and RP-HPLC (c). Black lines refer to 0 hr, red lines to 72 hr, blue lines refer to 192 hr of incubation. SDS-PAGE of an aliquot corresponding to 192 hr of incubation of E46K/DOPAC is also shown. The lines close to the gel bands indicate the position of proteins used as marker of molecular weight (66, 45, 36, 29, 24, and 20 kDa). The arrows in RP-HPLC chromatogram indicate the decrease of the intact protein and the increase of the aggregated and chemically modified species, respectively. Levels of oligomerization of E46K (up) in comparison to Syn (down) (b) calculated from the area under the peaks of size exclusion chromatography (SEC) chromatograms during incubation

catechols (Figure 3b). The formation of catechol-induced off-pathway oligomers appears promoted for E46K in higher extent than for Syn, especially in the early stages of incubation. Finally, DOPAC resulted more efficient than DOPET in inducing it. It is very likely that the inherent tendency to oligomerize associated with Glu-to Lys mutation is combined with a further effect of the catechol, which therefore exerts an additional effect.

The same samples were loaded in RP-HPLC (Figure 3c). In this case, the peak relative to the monomeric intact species in the presence of catechols decreased in intensity in favor of a new species eluted late in the chromatogram. This new species was previously characterized for Syn and it resulted to be an off-pathway oligomeric species.[36] In Table 1, the chemical characterization by mass spectrometry of the protein material corresponding to the main chromatographic peaks was shown. Chemical modifications were found in the oligomeric E46K eluting late in RP-HPLC, in line with what was observed for Syn. Hence, the overall behavior of E46K resembled that of Syn. However, the variant resulted less affected by the catechols and more prone to oligomerization.

2.3 | The conformation of the monomeric protein determines the extent of inhibition by catechols

Aimed at the investigation of large-scale conformational dynamics of E46K and Syn and the comparison of such dynamics in the absence and the presence of DOPAC and DOPET, we employed SEC to evaluate changes in the hydrodynamic volume of the proteins before and after the addition of each catechol at the same stages of aggregation. This parameter was correlated with the behavior of the protein as probed by native-MS and global HDX-MS. To highlight the differences between the protein species, taking into account the different rates of aggregation of E46K and Syn, the protein/catechol ratio of 1:5 was used and the time point at 48 r was chosen to compare the behavior of the proteins.

2.3.1 | Size exclusion chromatography

Figure 4 reported the SEC chromatograms relating to 0 and 48 hr, in comparison to the chromatogram acquired after 72 hr of incubation (already shown in Figure 3a) as a control. Before loading onto the column, the samples were ultra-centrifuged to remove insoluble particles from the aggregation mixture. At 0 hr of incubation, in the absence of catechols, E46K eluted with a volume of 15 ml, whereas Syn elution volume was 14.5 ml (Figure 4a$_1$, T 0, inset). This difference in the elution volume was previously considered statistically significant[23] and allows to correlate the increased compactness of the mutant in comparison to the wild-type protein, although both remained intrinsically disordered (Table 2). After 48 hr, in the absence of catechols, the elution volume of E46K decreased (14.6 ml) compared to time 0, suggesting a slight but significant increase in the protein hydrodynamic volume upon incubation. This value was constant up to 72 hr of incubation, when only a reduction of the

TABLE 1 Chemical characterization of E46K in the absence and in the presence of DOPAC and DOPET (Figure 3c)

			Molecular mass (Da)		
DOPAC	**Time (hr)**	**RT (min)[a]**	**Found[b]**	**Calculated[c]**	**Protein species**
E46K	0	21.5	14,459.41 ± 0.12	14,459.24	E46K
	72	21.5	14,459.35 ± 0.10	14,459.24	E46K
		32.5	14,580.61 ± 0.46	14,580.24	E46K + 121 Da
	192	32.5	14,580.81 ± 0.86	14,580.24	E46K + 121 Da
			Molecular mass (Da)		
DOPET	**Time (hr)**	**RT (min)[a]**	**Found[b]**	**Calculated[c]**	**Protein species**
E46K	0	21.5	14,459.25 ± 0.20	14,459.24	E46K
	72	21.5	14,459.25 ± 0.02	14,459.24	E46K
		32.5	14,590.81 ± 0.96	14,590.24	E46K + 131 Da
	192	32.5	14,590.19 ± 1.49	14,590.24	E46K + 131 Da

Abbreviations: DOPAC, 3,4-dihydroxyphenylacetic acid; DOPET, 3,4-dihydroxyphenylethanol.

[a]Protein species are listed in order of retention time (RT).

[b]Experimental molecular masses determined by ESI-QTOF-MS.

[c]Molecular masses calculated from Syn amino acid sequence.

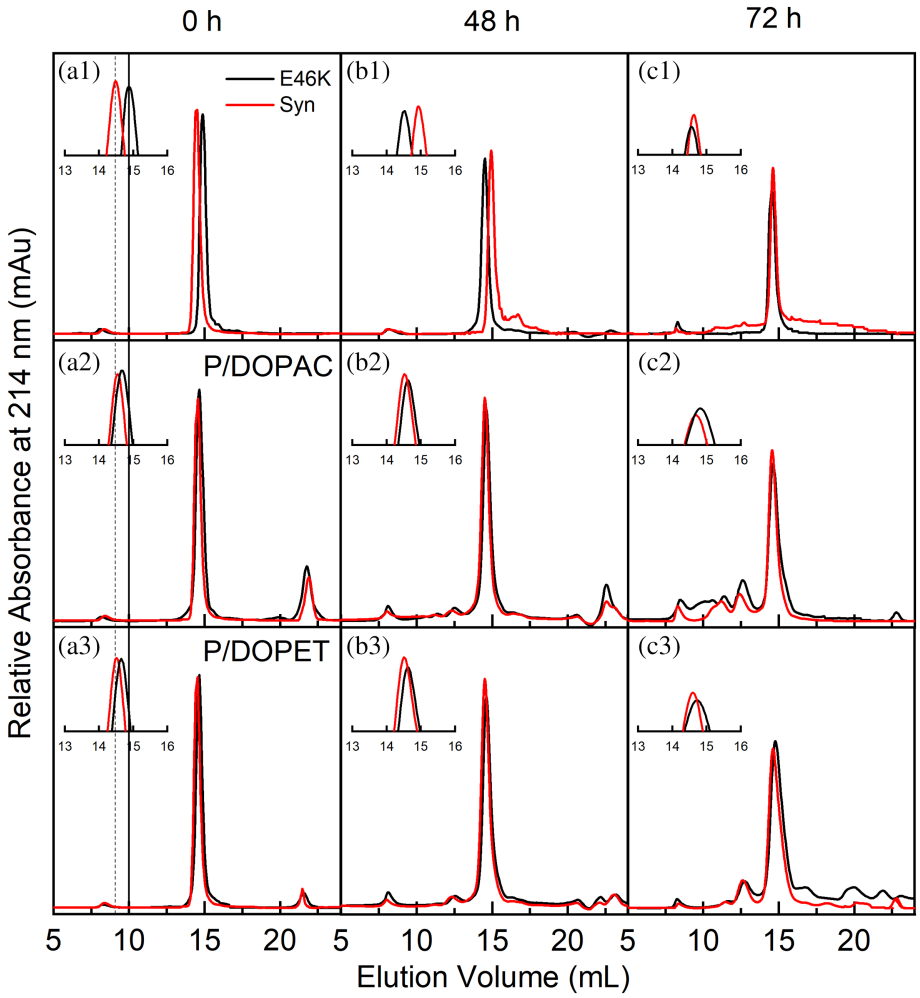

FIGURE 4 Size exclusion chromatography (SEC) analyses of E46K (black lines) and Syn (red lines) upon 0 (a), 48 (b), and 72 (c) hr of incubation under shaking in the absence (a_1, b_1, c_1) and in the presence (a_2, b_2, c_2) of 3,4-dihydroxyphenylacetic acid (DOPAC) and (a_3, b_3, c_3) of 3,4-dihydroxyphenylethanol (DOPET). Inset: zoom of the SEC chromatograms evidencing the difference in elution volumes

intensity of the peak is observed. In the case of Syn, the trend is the opposite: the elution volume shifted from 14.5 ml at time 0 to 14.9 ml at time 48 hr and to 14.6 ml at time 72 hr. In the presence of DOPAC, at time 0, E46K showed a minor elution volume in SEC (14.6 ml) than the ones shown in the absence at the same time point, suggesting a catechol stabilizing effect of a more extended conformer. The addition of DOPET induced a similar effect. Leaving the samples in the presence of catechols, E46K elution volume did not exhibit variations (Figure 4b_2–c_2, b_3–c_3; T 48 and 72 hr, and Table 2). Another effect induced by the presence of the catechols in the samples was an enlargement of the chromatographic peak, which is indicative of the presence of new protein species. In the case of Syn, its elution volume upon addition of catechol did not change over time (14.6 ml).

2.3.2 | Native-MS

Samples of E46K and Syn proteins collected by SEC after 0 and 48 hr of incubation with or without DOPAC and DOPET were further analyzed by Native-MS to monitor protein ion charge-state distribution. As the extent of multiple charging of protein ions in ESI-MS is determined by their solvent-exposed area, the charge-state distributions depend on conformation in solution. Typically, more compact conformers give rise to ions with relatively low charge density and appear in the high m/z region of the spectra, while partially or fully unstructured protein molecules are able to accommodate a significantly higher number of charges due to an increased surface area. If multiple compact and denatured states of the protein coexist at equilibrium in solution, the protein charge-state distributions are multimodal. Representative ESI-MS spectra of E46K (left) and Syn (right) in the absence of catechols were reported in Figure 5a showing the coexistence of three populations, indicated as 1, 2 and 3, corresponding to multiple conformers with different compactness. As represented in Figure 5b, Population 1 corresponds to the most relaxed conformation and Population 3 to the most compact one, according to their m/z values. Population named 2, with intermediate properties, resulted to be the most abundant for both E46K and Syn.

TABLE 2 E46K and Syn parameters calculated by SEC (Figure 4), and HDX (Figure 6) measurements

			Incorporated deuterons[b]			
Species	**Time (hr)**	**Elution volume (ml)[a]**	**10 s**	**1 min**	**10 min**	**70 min**
E46K	0	15.0	75 ± 0.08	80 ± 0.13	94 ± 0.09	96 ± 0.02
E46K/DOPAC	0	14.6	88 ± 0.12	91 ± 0.09	95 ± 0.12	98 ± 0.05
E46K/DOPET	0	14.6	82 ± 0.23	83 ± 0.22	94 ± 0.21	98 ± 0.08
E46K	48	14.6	75 ± 0.26	80 ± 0.23	94 ± 0.08	96 ± 0.11
E46K/DOPAC	48	14.6	89 ± 0.39	91 ± 0.44	94 ± 0.09	98 ± 0.08
E46K/DOPET	48	14.6	81 ± 0.19	84 ± 0.31	93 ± 0.11	98 ± 0.03
E46K	72	14.6	n.d.			
E46K/DOPAC	72	14.6	n.d.			
E46K/DOPET	72	14.6	n.d.			
Syn	0	14.5	80 ± 0.31	83 ± 0.29	96 ± 0.19	98 ± 0.12
Syn/DOPAC	0	14.5	82 ± 0.29	90 ± 0.33	99 ± 0.38	100 ± 0.07
Syn/DOPET	0	14.5	81 ± 0.13	94 ± 0.25	96 ± 0.18	100 ± 0.03
Syn	48	14.9	80 ± 0.19	83 ± 0.26	96 ± 0.15	98 ± 0.02
Syn/DOPAC	48	14.6	82 ± 0.42	90 ± 0.22	98 ± 0.17	101 ± 0.22
Syn/DOPET	48	14.6	80 ± 0.59	94 ± 0.26	97 ± 0.19	101 ± 0.02
Syn	72	14.6	n.d.			
Syn/DOPAC	72	14.6	n.d.			
Syn/DOPET	72	14.6	n.d.			

Abbreviations: DOPAC, 3,4-dihydroxyphenylacetic acid; DOPET, 3,4-dihydroxyphenylethanol.

[a]All data were performed eight times with an error of ±0.2 ml.

[b]All data were performed in triplicates with an error of ±1 Da due to the software limits. The single standard deviations are represented as ±SD.

To evaluate the conformational effects induced by the catechols on the proteins, we acquired spectra of samples obtained by incubating either DOPAC or DOPET with each protein for 0 and 48 hr. Signal intensities of the various conformational states were utilized to quantify the relative percentage of each observed population (see Methods sections for details). The histograms in Figure 5c show that in the absence of catechols (gray columns), differently from Syn, E46K populated at higher extent a more compact conformation (3) than the more extended one (1), according to our previous results. The presence of DOPAC (dark purple columns) shifted the equilibrium toward a slightly more relaxed conformation, as depicted from the increase of the percentage of population 1 at the expense of population 3. This effect resulted to be more evident for Syn rather than for E46K. However, it is striking to note that the increase of E46K extended Population 1 occurred at the expenses of the compact 3, whereas in the case of Syn, Population 2 decreased upon the addition of DOPAC. The DOPET-induced effects on E46K resulted to be quite similar to those induced by DOPAC on Syn, producing only a slight redistribution of conformers with the increased abundance of Population 1 at the expenses of 2. The presence of DOPET in the Syn sample, instead, did not significantly alter the population equilibria.

After 48 hr of incubation in the absence of catechols (gray columns), the abundance of the relaxed Population 1 of E46K increased, suggesting a loss of compactness. In the case of Syn, we observed an opposite effect. This is consistent with the fact that the rate of aggregation is faster for E46K and therefore, at 48 hr-incubation, the two proteins, which exhibit different kinetics of aggregation, were found in a different conformational state. Moreover, the two proteins resulted to be differently affected by the catechols. When E46K is incubated with DOPAC for 48 hr, the protein compactness increases, according to the substantial increase in Population 3, at the expense of the other population. The effect is more evident adding DOPET (light purple columns), with a further increase in the protein compactness. This could be explained considering a protective effect of catechol that shielded the protein exposed regions. On the contrary, being Syn in a previous step of oligomerization in comparison to E46K, Population 1 is slightly more abundant when incubated with catechols. Indeed, the

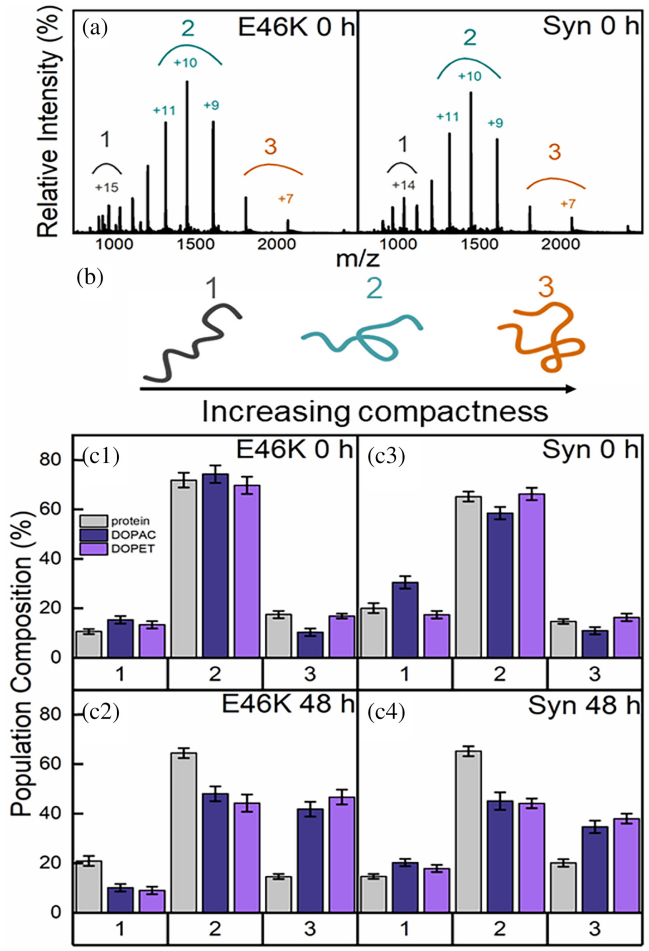

FIGURE 5 Native-MS measurements. ESI-MS spectra of samples containing 10 μM of E46K (left) and Syn (right). The numbers 1, 2 and 3 indicate three different populations (a). Graphical representation of the conformers with different compactness detected simultaneously in solution by native MS (b). Histograms comparing the percentages of each population observed for E46K (c_1, c_2) and for Syn (c_3, c_4) in the absence and in the presence of 1:5 catechol at time 0 (c_1, c_3) and after 48 hr incubation (c_2, c_4). Gray columns refer to the proteins in the absence of catechol, the dark and light purple refer to the proteins in the presence of 3,4-dihydroxyphenylacetic acid (DOPAC) and 3,4-dihydroxyphenylethanol (DOPET), respectively.

catechol-shielding effect appears less visible. Finally, in line with previous analysis, DOPAC resulted to be more efficient than DOPET in inducing conformational change effects in both proteins.

2.3.3 | HDX-MS

In HDX-MS approach, backbone amide hydrogens of the polypeptide chain undergo rapid isotopic exchange with the solvent in dynamic regions lacking persistent internal hydrogen bonds, whereas regions with backbone amides engaged in stable interactions are protected against the exchange. We analyzed under the same experimental conditions, the species eluted from SEC column after 48 hr of incubation in the presence of each catechol as well as the native and monomeric proteins. In Figure 6a, the deconvoluted electrospray ionization mass spectra obtained from undeuterated and deuterated samples were reported. The nontreated E46K and Syn monomer profiles were shown (black lines) as a control. The same profiles produced by global HDX-MS in an isotopic exchange time of 10 s, 1, 10, and 70 min were reported. After 10 s of incubation (red lines) in deuterated buffer at pH 7.4 and on ice, a mass shift of 75 ± 0.08 and 80 ± 0.31 Da (equivalent to incorporation of ~75 and 80 deuterons) was observed for E46K and Syn, respectively. To obtain the complete deuteration of the molecules, the measurements were done up to 70 min, observing a mass shift of 96 ± 0.02 and 98 ± 0.12 for E46K and Syn, respectively. The samples were left in deuterated solvent for 100 min at room temperature to verify whether 70 min on ice were sufficient to obtain the complete exchange. The number of exchanged D, calculated under this condition, did not increase even though deuteration was prolonged. Overall, in the absence of catechols, E46K exhibited a rate of exchange slightly lower than Syn (Figure 6b), especially in the early steps of deuteration (1–60 s. This suggests that more protected and compact conformers populate E46K at this stage. Of interest, at short incubation times with deuterium, for both proteins more populations seem to exist at equilibrium, with different rate of exchange, corresponding to different number of exchanged deuterons, therefore to different exposure of the conformers to the solvent. After that, the measurements were conducted on E46K and Syn species (M*) deriving from incubation for 48 hr with catechols. In the presence of DOPAC, E46K exchanged slightly faster than in the absence of the catechol both at 0 and 48 hr. After 10 s, in E46K the number of incorporated deuterons passed from 75 in the absence to 89 in the presence of DOPAC (Table 2), similarly to the wild-type protein. Indeed, the difference between the exchanged deuterons in the absence and in the presence of DOPAC is less evident in Syn (81 vs. 82 exchanged D) since the wild-type protein started from an already more relaxed conformation in respect to the mutant. According to the results obtained by the other techniques, DOPAC seems to have a major effect on the two proteins than DOPET. Figure 6c showed the different D exchange rates of the proteins. In the absence of catechols, this difference is statistically relevant in all time points and particularly evident in the first stages of exchange. In the presence of catechols, at 10 s E46K exchange rate was faster, while progressively, a minor difference was observed between

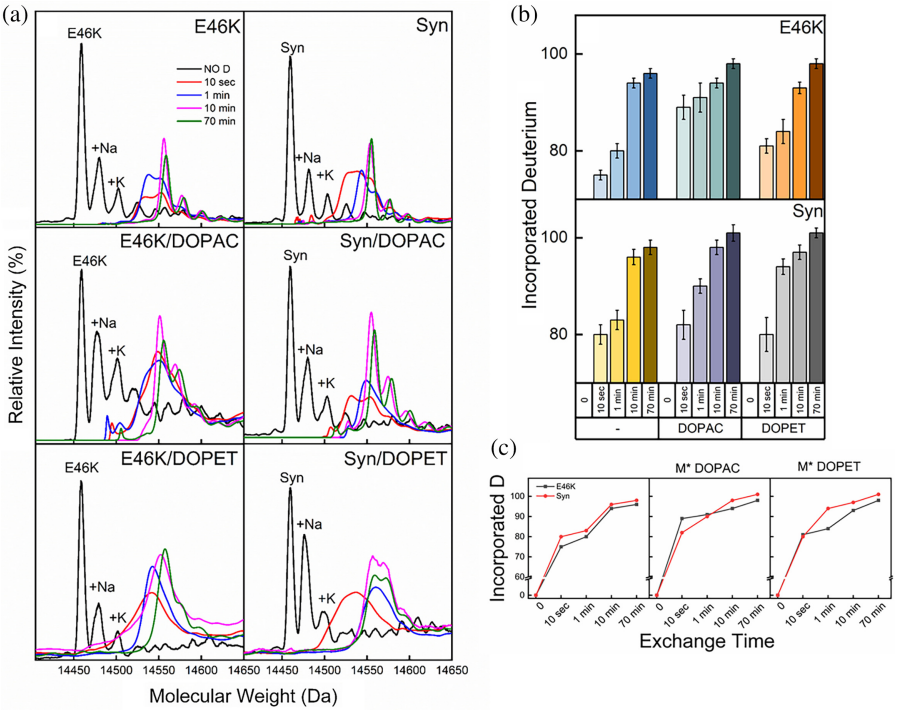

FIGURE 6 HDX-MS experiments. Deconvoluted mass spectra (a) of E46K (left) and Syn (right) obtained from undeuterated (black lines) and deuterated samples after incubation for 10 s (red line), 1 min (blue line), 10 min (pink line) and 70 min (green line). Number of incorporated deuterons in E46K and Syn in the absence and in the presence of catechols during incubation (b). Number of incorporated deuterons plotted as a function of the exchanged time (c)

the two proteins, especially at 70 min. At this step, both curves, having a logarithmic trend, tend to their maximum limit.

2.4 | DOPAC and DOPET disaggregate preformed oligomers and fibrils at different extent

To ascertain whether DOPAC and DOPET bind the aggregated forms produced during the protein aggregation, an experiment of disaggregation was carried out. The catechol was added to aliquots of protein samples collected from the aggregation mixtures after 48 and 168 hr of incubation. It was used a ratio of 1:5 (protein/catechol) maintaining the same conditions used for the aggregation experiments. The process was monitored by ThT fluorescence and the emission spectra obtained for E46K in the absence of DOPAC were reported for the time points 0, 48, and 168 hr (Figure 7a, black lines). The aliquots corresponding to 48 hr of incubation were divided in two fractions and one was left to aggregate and the other was treated with DOPAC. After 1 day (+24 hr) of incubation, an increase of ThT fluorescence was observed for the sample of E46K incubated in the absence of DOPAC (black line, 48 + 24 hr), while for the other one a decrease of the fluorescence intensity was detected (red line, 48 + 24 hr + DOPAC). The same procedure was followed for the fraction collected at 168 hr, and in this case, E46K aggregates appeared slightly affected by the catechol (black line 168 + 24 hr; red line 168 + 24 hr + DOPAC). DOPET induced similar effect but in a minor extent (data not shown). In the case of Syn (Figure 7b), the catechol was added at 48 hr when the protein was in a different stage of aggregation than E46K. As detected by native-MS and SEC, Syn populated prevalently a more compact conformer in respect to its mutant. The fibril formation was inhibited when DOPAC was added to the aggregation mixture at 48 hr; indeed, no increase of ThT signal was observed (Figure 7b, red line, 48 + 24 hr + DOPAC). At 168 hr, ThT fluorescence had a similar trend and the spectra appeared almost superimposable (black line 168; red line 168 + 24 hr + DOPAC).

The species obtained adding the catechol to preformed aggregates (48 hr) or fibrils (168 hr) were characterized by TEM. In Figure 7c, the comparison between the morphology of E46K species before (c_1 and c_3) and after the addition (c_2 and c_4) of DOPAC was shown. At 48 hr, E46K generated several species as expected at the beginning of the growth phase of fibrillation (Figure 7c_1). They are compatible with oligomers and short fibrils.[39] The oligomers measured diameters ranging 8–13 nm, while the nascent fibrils 10–15 nm. These species disappeared from the aggregation mixture upon adding DOPAC (1:5 ratio) and new types of aggregates were detected by TEM (Figure 7c_2). A heterogeneous population of species is detectable: spherical oligomers and amorphous aggregates coexist. In this sample, short and broken fibrils (diameter 6–11 nm) are still present. In the sample where the protein was left aggregating for 168 hr

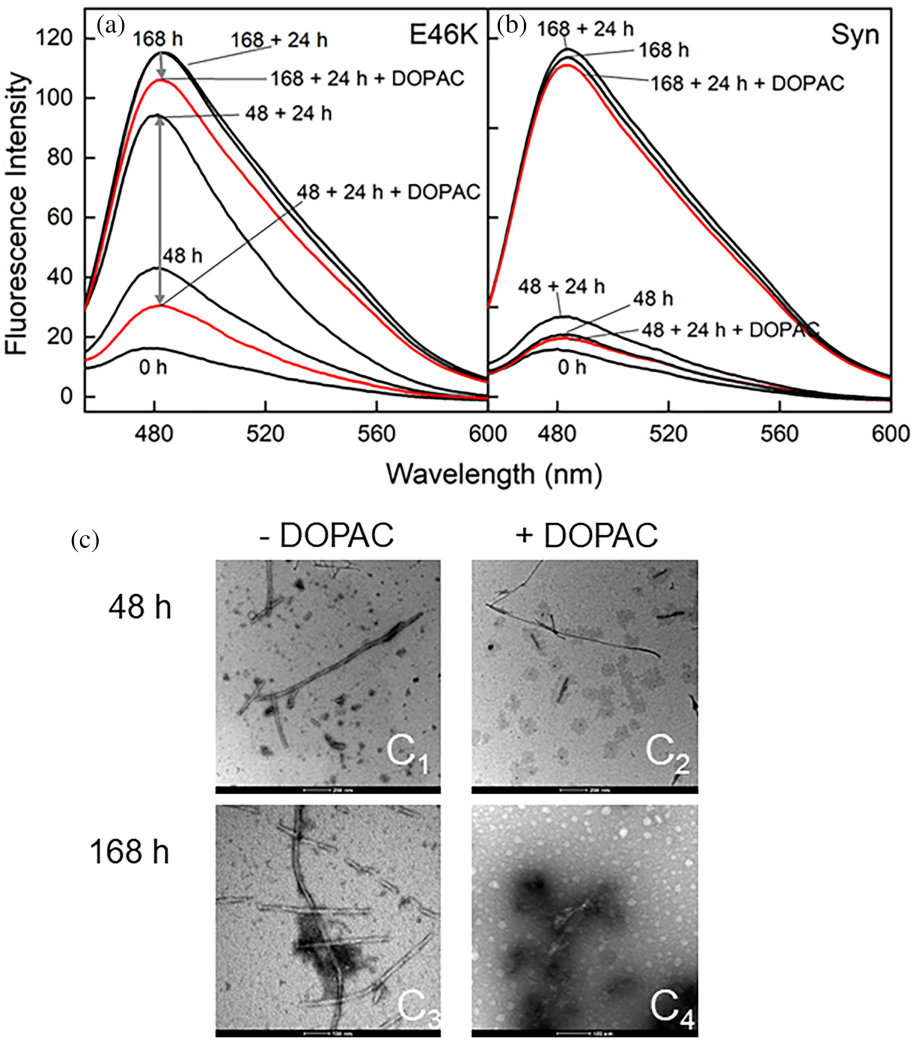

FIGURE 7
3,4-Dihydroxyphenylacetic acid (DOPAC)-induced E46K (a) and Syn (b) disaggregation probed by ThT fluorescence. Aliquots were collected from the aggregation mixture after 48 and 168 hr of incubation in the absence of catechol, then DOPAC was added at a 1:5 final protein/DOPAC ratio. Measurements were collected after further 24 hr of incubation. Black ThT spectra correspond to 0, 48, 72, 168, 192 hr of aggregation. In the picture, the 72 hr-sample is indicated as 48 + 24 hr and the 192 hr-sample is indicated as 168 + 24 hr. Red ThT spectra refer to 48 and 168 hr of aggregation plus 24 hr of incubation in the presence of DOPAC. TEM images (c) taken from E46K samples corresponding to 48 and 168 h of incubation in the absence (−) and after the addition of DOPAC (+). The scale bars are 200 nm (c_1–c_2) and 100 nm (c_3–c_4).

in the absence of DOPAC (Figure 7a, black line), E46K fibrils were found (Figure 7c_3). The TEM measurements conducted on the E46K/DOPAC mixture at 168 + 24 hr after the addition of the catechol showed the formation of off-pathway aggregates with a morphology similar to the species formed at 48 + 24 hr after the addition of DOPAC. In this case, the morphology appeared more defined with diameters ranging 15–30 nm (Figure 7c_4). Rare and broken fibrils are still present. These residual fibrils probably derive from the degradation of pre-formed fibrils as suggested from the decrease of the ThT intensity. TEM pictures relative to Syn were reported in Figure S2 as a comparison.

3 | DISCUSSION

There is strong evidence that the monomeric Syn, in vitro at physiological conditions, populates an ensemble of conformations ensuing from its rugged folding energy landscape.[40] Slightly extended conformers and structures that appear more compact than expected coexist in solution. Biophysical studies proposed that these partially folded structures of Syn can derive from transient electrostatic and hydrophobic interactions between the positively charged N terminus and the negatively charged C terminus, and also between the NAC region and the C terminus.[40,41] In native conditions, these interactions continuously open and close conferring to Syn the required flexibility to interact with different partners in vivo.[41] However, these dynamic interactions can lead, in turn, to conformations that trigger protein aggregation pathways.[42] The identification and the confinement of aggregation-prone conformations and/or the stabilization of the aggregation not-prone ones might be targets of possible therapeutic intervention.

Multiple studies link the inherent dynamics of E46K mutant of Syn to different onset and development of PD pathogenesis. Especially, E46K variant develops species more toxic than the wild type Syn,[15,21,43] an important issue is therefore to know whether a targeting Syn drug would be effective also against its genetic mutants.

Herein, we have studied how DOPAC and DOPET affect the ability of E46K variant of Syn to form fibrils, comparing side by side these results with those obtained with the wild-type protein. We show that E46K and Syn aggregation is inhibited by catechols in a dose-dependent manner. E46K requires higher concentrations of DOPAC and DOPET for its complete inhibition than Syn. Moreover, DOPAC appears more efficient than DOPET in inhibiting amyloid formation. Finally, the protein dynamics and surface exposure appear critical for the catechol/protein interaction.

We focused on the conformations populated by Syn and E46K at the initial stages (0–48 hr) of the aggregation process, when in the case of E46K, the monomer–oligomer equilibrium appears more shifted toward the aggregated species due to the higher rate of aggregation experienced by the mutant.[17,23] By using native and HDX-MS, we show that, although three main conformations are evident for both proteins, their ratio is different and DOPAC and DOPET induce a marked redistribution of these conformations affecting their equilibrium. As summarized in Figure 8, our data reveal the co-existence of an extended and relaxed species (indicated with 1), a fairly compact one (3) at the opposite edge of the equilibrium, and a species with intermediate properties (2). This last is highly represented in both proteins, due probably to the rapid interconversion between the species at room temperature. However, it is possible to appreciate that the extreme species appear differently populated by Syn and E46K. At Time 0, the compact conformer (3) of E46K seems to be more populated at the expenses of the relaxed one (1), accordingly to Fredenburg et al.[23] These data are corroborated by the behavior of the protein in SEC, where a larger elution volume; therefore, a lesser hydrodynamic radius of E46K than Syn was found. Consistently, E46K also exhibits a reduced exposure to solvent as probed by hydrogen/deuterium exchange of the protein backbone.

The ratio between the compact and extended species changes during incubation. After 48 hr-aggregation, the fraction of E46K in open conformation increases, while Syn seems to undergo compactness. This phenomenon is strongly correlated with the presence of the amyloidogenic mutation that speeds up the aggregation of the mutant.[18] The intramolecular unfolding of the loosely packed structures is an essential step occurring prior to protein aggregation to expose the aggregation-prone regions of the protein.[40,44] On the other hand, incubating the proteins in the presence of the catechols, a significant change in the relative ratio of the conformers occurs with an increase of the relaxed conformation in both proteins. This clearly suggests that the catechols, especially DOPAC, could prevent the long-range

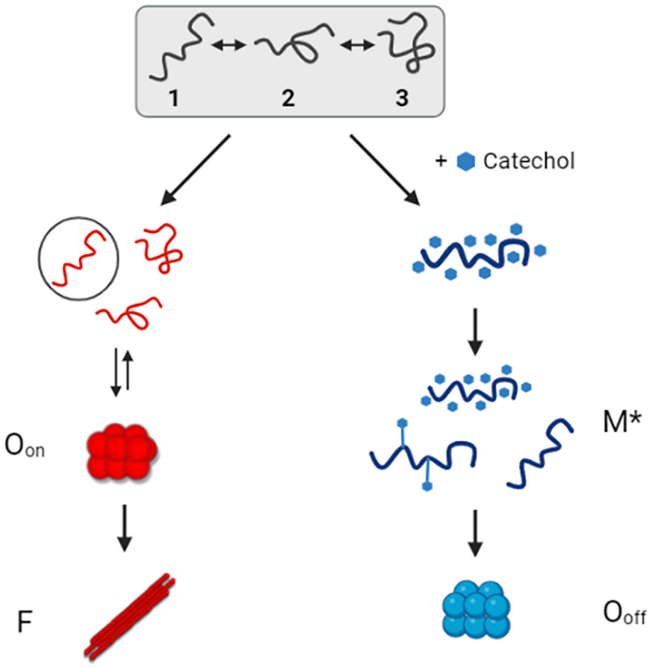

FIGURE 8 Schematic representation of the ensemble of conformations populated by Syn and its mutant E46K (up). Three populations, indicated as 1, 2, and 3, were identified corresponding to multiple conformers with increasing compactness. In the absence (left) of catechols, among the interconverting species, the more aggregation-prone one undergoes nucleation events followed by the formation of intermediate transient forms, named on-pathway oligomers (O_{on}) that culminate in fibrils (F). In the presence (right) of catechols, the species with higher affinity for these molecules bind them through noncovalent and covalent binding giving rise to modified monomer, M*, that then generate off-pathway harmless oligomers, O_{off}.

interactions in Syn molecules responsible for the packed conformations, establishing new interactions. At the beginning, these protein/catechol interactions stabilize the extended conformation that seems to exhibit the higher affinity for the metabolite. Successively DOPAC and DOPET generate a shield around the molecule hiding the side chain of certain residues and hampering the intramolecular aggregation process. This would provide an explanation for the reduced efficiency of catechols toward E46K. In fact, being higher the concentration of the compact conformer in E46K or higher the rate of interconversion of the two species, the required catechol amount is higher.

Since different processes take place in solution, after 48 hr-incubation in the presence of catechols, this study focused on the events occurring within this time point. Indeed, prolonging the incubation, off-pathway oligomers (especially E46K) are generated, and in particular dimers and trimers were observed. These species have

been previously isolated and characterized in terms of structure and cytotoxicity, and interestingly they exhibit reduced cytotoxicity and ROS production. Moreover, DOPAC-induced oligomers activate lysosomal activity favoring the clearance of Syn aggregates and attenuating Syn build-up within Syn-exposed cells. Finally, they reduce the ability of Syn to interact with lipid membranes.[35,37] In this study, HDX-MS and SEC data show that the monomer opening effect induced by catechols is preserved during aggregation and a significant fraction of extended and relaxed conformation is maintained. Additionally, the native-MS data indicate an increase in the compact population. Actually, this species adopts fewer charges in mass spectrometry (higher m/z) and its increase could derive from a combined effect of chemical modifications of the side chain of the protein and catechol polymerization that provide a shield of the protein, that at this stage acquires less charges. In conclusion, the catechols stabilize the more relaxed conformation confining it in a nonaggregating species.

Our results provide evidence that the mechanism of interaction of DOPAC is different from that of DOPET due to its intrinsic chemical structure. DOPAC binds Syn and E46K mainly by electrostatic interactions for the presence of the negatively charged carboxyl moiety. In solution, the positive charges of Syn could be neutralized and, consequently, the long-range interactions between the N and C-terminal regions and NAC and C-terminal of the protein cannot be formed.[41] Similarly, the Syn backbone electrostatic association can be skewed by adding salt ions.[45] However, this provides an opposite effect at the level of the long-range electrostatic contacts, favoring the hydrophobic interactions and driving Syn to aggregation. As matter of fact, DOPAC might compete with the aromatic π–π interactions that seem to deeply contribute to the fibril formation events in Syn.[44] The dihydroxyphenolic moieties of the catechol layering at the interface between the molecules increase the protein solubility. This is corroborated by the observation that in the presence of DOPAC, by HDX-MS, the protein exchanges faster, suggesting a higher solvent exposure of the protein backbones. Conversely, the interaction of the protein with DOPET is mediated by weaker electrostatic forces due to the alcoholic less nucleophile OH than the carboxyl group. Indeed, the packed conformations generated in the presence of DOPET appear more populated than in the presence of DOPAC. Summing up, the shield generated by DOPAC competes with the intermolecular and intramolecular interactions, favoring the formation of protected conformation that does not proceed in the fibril formation.

To further demonstrate the higher affinity of catechol for the relaxed conformation of Syn, an experiment of disaggregation was done and DOPAC or DOPET (1:5) were added to E46K and Syn, which were left to incubate for 48 hr. The decrease of ThT signal intensity was clearly seen for E46K, whereas the fluorescence intensity was the same in the case of Syn. It must be underlined that at 48 hr, the native-MS measurements had shown that E46K populates in a relatively higher extent the relaxed conformation at variance with Syn, whose compact conformers were formed at the expense of the more extended one. Therefore, the catechols seem to block Syn aggregation interacting with the reduced fraction of open conformation and barely affecting the process. On the contrary, they exert a disaggregating effect when they were added to E46K mixture at 48 hr, where the major species is the extended one. These data provide further evidence that the different abilities of the protein to be affected by catechols derive from the initial equilibrium between the different conformers of the proteins.

Several strategies were proposed for the prevention of Syn toxicity and to counteract PD precisely targeting the protein. The possibility to interfere with Syn oligomer and fibril formation, considered as the major pathogenic process in Parkinson disease, is particularly attractive. Since Syn and its familial mutants do not have a single, major conformation, but appear as a dynamic ensemble of conformations with similar energies, the rational design of drugs based on the knowledge of the structure of the target protein, in this case, is not applicable and the development of therapeutic strategies based on the recognition of the active site of Syn is a difficult task. Increasing the stability of species in their native and harmless state or the kinetic barrier to form misfolded species by using small molecules would be a great leap forward in medicinal chemistry, leading to an expansion of the druggable genome.

The most compelling argument in favor of the use of small molecules able to stabilize Syn stems from the numerous examples of natural products such as Oleuropein aglycone tested by us showing that it prevents the formation of toxic Syn species inducing new and harmless oligomers[35] and by others on other amyloidogenic molecules.[46,47] By using surface plasmon resonance high-throughput screening, Toth et al.[48] have identified novel, completely synthetic, Syn interacting drug-like compounds able to rescue Syn malfunctions and to inhibit the protein aggregation, without inducing changes in its conformation. Another class of compounds is given by molecules such as squalamine capable of competing with Syn in native and aggregated form for the lipid membrane binding and reducing their toxicity.[49] DOPAC and DOPET are interesting candidates as scaffolds for the synthesis of new molecules able to antagonize the formation of fibrils. However, their use shows

some limitations like low bioavailability, nonlinear pharmacokinetic behavior, and pharmacodynamics problems, and therefore there are still many questions to be clarified and precise knowledge of their mechanism of action would provide the possibility of producing pharmacologically more effective molecules with ameliorate pharmacodynamics properties.

In conclusion, our findings provide insights into the aggregation mechanism of Syn and its mutants and suggest the possibility to modulate this process by compounds containing a catechol scaffold. By using dynamic biophysical approaches, we provided evidence that these molecules interact differently with the interconverting conformers of monomeric Syn and its familial variant E46K in solution, stabilizing the best-fitting conformation and selecting the most prone-to-aggregation one, confining it into an off-pathway oligomer. Therefore, catechol-containing molecules could represent potential therapeutic agents for PD and other pathologies associated with Syn amyloidogenic properties.

4 | MATERIALS AND METHODS

4.1 | Materials

DOPAC, DOPET, Thioflavin T (ThT), and lyophilized bovine catalase (CAT) were purchased from Merck (Darmstadt, Germany). The catechol powder was dissolved in water solution at 100 mM final concentration and stored at −20°C.[50] All reagents and chemicals were obtained from Sigma or Fluka (St. Louis, MO, USA) and were of analytical reagent grade.

4.2 | Expression and purification

The expression of α-Synuclein (Syn) was conducted in *Escherichia coli* BL-21 while for the E46K mutant expression *E. coli* BL-21 Gold cells were used. The purification of the recombinant protein was conducted following a procedure previously described.[51] Protein identity and integrity were assessed by mass spectrometry (MS).

4.3 | Protein fibril formation and disaggregation

Protein samples (70 μM), filtered with a 0.22 μm pore-size filter (Millipore, Bedford, MA, USA) were incubated at 37°C in 20 mM sodium phosphate buffer, pH 7.4 up to 7 days under shaking at 750 rpm with a thermo-mixer (Compact, Eppendorf, Hamburg, DE) in the absence (control) or in the presence of DOPET or DOPAC by using molar protein/substance ratios of 1.1, 1:2, 1:5. To avoid the catechol-induced oxidation of methionine residues, catalase was added to the aggregation buffer.[36] Aliquots were collected at the indicated incubation time and the formation of fibril was checked by ThT binding assay, transmission electron microscopy (TEM), and circular dichroism (CD). The ThT binding assay was performed according to LeVine,[52] using a 25 μM ThT solution in 25 mM sodium phosphate buffer, pH 6.0. Fluorescence emission measurements were performed at 25°C exciting at 440 nm and recording the ThT fluorescence in the 455–600 nm interval. To evaluate eventual interferences of catechols on ThT assay, DOPET and DOPAC fluorescence was measured as a control.

The disaggregation effect of DOPAC and DOPET of pre-made Syn and E46K aggregates was tested by ThT and TEM, adding the catechols to the aggregation mixture at 48 and 168 hr of incubation, corresponding to steps enriched in on-pathway oligomers or fibrils, respectively. For this experiment, 48 hr or 168 hr-aged samples were incubated with DOPAC or DOPET (at a final concentration of 1:5/protein: catechol) at 37°C under shaking at 750 rpm, for further 24 hr. All aggregate concentrations were expressed as monomer protein concentration.

4.4 | Aggregate morphology analysis

The morphology of the protein aggregates was characterized by TEM. Negative staining was performed by placing a drop of the sample solution on a Butvar-coated copper grid (400-square mesh) (TAAB-Laboratories Equipment Ltd, Berks, UK). Then, the sample was dried and negatively stained with a drop of uranyl acetate solution (1.0%, w/v). TEM pictures were taken on a Tecnai G2 12 Twin instrument (FEI Company, Hillsboro, OR) at an excitation voltage of 100 kV. Many pictures were collected at different magnifications. Image J software was used to get size information. Size distribution of protein species was calculated on 200 particles manually extracted from the micrographs. Only clearly defined spherical and isolated particles were selected. The species with diameters larger than 100 nm were excluded. Measurements were obtained with a standard deviation of ±8.

4.5 | Chemical–physical characterization

Size exclusion chromatography (SEC) was performed by a Superdex TM 200 Increase (10/300 GL) column

(Amersham Biosciences, Uppsala, Sweden), using an ÄKTA FPLC system (Amersham Biosciences, Uppsala, Sweden). Sample aliquots (200 µl) were withdrawn from the aggregation mixture, centrifuged, loaded onto the column and eluted at 0.75 ml/min in 20 mM Tris–HCl buffer, pH 7.4, containing 0.15 M NaCl. The effluent was monitored by recording the absorbance at 214 nm. Column calibration was obtained using the following standards: blue dextran (void volume); albumin, 67 kDa; ovalbumin, 45 kDa; α-lactalbumin, 14.4 kDa and aprotinin, 6.5 kDa. The RP-HPLC analyses were carried out on an Agilent 1200 chromatographer (Santa Clara, CA) using a Jupiter C18 column (4.6 × 250 mm; Phenomenex, CA, USA), eluted with the following gradients of acetonitrile/0.085% TFA–water/0.1% TFA: 5–25%, 5 min, 25–28%, 13 min, 28–39%, 3 min, 39–43%, 21 min or 5–38%, 5 min, 38–43%, 15 min. The effluent was monitored by recording the absorbance at 226 nm. The identity of the eluted material was assessed by mass spectrometry. SDS-PAGE was performed with a Mini-PROTEAN II Bio-Rad electrophoresis system using a Tris–HCl 13% (w/v) polyacrylamide gel. The bands were stained by Coomassie Brilliant Blue. Approximately 4 µg of protein was loaded into each well. Mass spectrometry analysis was carried out with an electrospray ionization (ESI) mass spectrometer equipped with a Q-Tof Xevo G2S (Waters, Manchester, UK). Measurements were carried out at 1.5–1.8 kV capillary voltage and 30–40 V cone voltage.

4.6 | Spectroscopic characterization

Protein concentrations were determined by absorption measurements at 280 nm using a double-beam Lambda-20 spectrophotometer (Perkin Elmer Life Sciences). The molar absorptivity at 280 nm for Syn and E46K samples was 5,960 cm^{-1} M^{-1}, as evaluated from their amino acid composition by the method of Gill and von Hippel.[53] Secondary structure conformation of E46K and wild-type protein was assessed by far-UV circular dichroism (CD). The measurements were performed on a J-800 Series spectropolarimeter (JASCO, Japan) in a 1-mm quartz cuvette at room temperature. Data were collected in the wavelength range of 250–190 nm. All protein samples were measured at the same settings averaged in five and the buffer data subtracted. Only data with high-tension voltage <600 V were collected and shown to avoid too noisy signals. The mean residue ellipticity [θ] (degree cm^2 $dmol^{-1}$) was calculated from the formula [θ] (θ_{obs}/10) (MRW/lc), where θ_{obs} is the observed ellipticity in degrees; MRW is the mean residue molecular weight of the protein; l is the optical path length in cm; and c is the protein concentration in g/ml. A protein concentration of 7 µM was used. The spectra were recorded in 25 mM sodium phosphate buffer pH 7.4.

4.7 | Native MS

E46K and Syn samples, in the absence and in presence of catechols (protein/catechol = 1:5) collected from SEC at time points 0 and 48 hr were buffer exchanged by filtration using Amicon Ultra-0.5 centrifugal filters (Merck Millipore Ctd, Ireland) to minimize the presence of salts that can adversely interfere with ESI performance. Samples, diluted in 200 mM ammonium acetate (pH 7.0) to achieve a final 10 µM protein concentration, were analyzed by direct infusion electrospray ionization (ESI) on a Q-Tof Xevo G2S spectrometer (Waters). The analyses were performed in nanoflow mode by using quartz emitter produced in-house by using a Sutter Instruments Co. (Novato, CA, USA) P2000 laser pipette puller. Up to 5.0 µl samples were typically loaded onto each emitter by using a gel-loader pipette tip. A stainless-steel wire was inserted in the back end of the emitter to supply an ionizing voltage in the range of 1–1.6 kV. Source temperature was set at 30°C and desolvation voltage was 40 V. All experiments were performed in positive ion mode. Data were processed by using Mass Lynx (v 4.2, SCN781; Waters) software. To evaluate conformer occurrence, abundances of the different populations in each experiment were calculated aided by in-house developed MATLAB (R2016b) scripts, expressed as percentage, and compared.

4.8 | HDX experiments

HDX experiments[54] were performed on protein samples eluted by SEC at a final concentration of 0.1 µM. H/D exchange was performed diluting samples 20 folds in deuterated buffer (20 mM sodium phosphate pH 7.4 in deuterated water) to a final D_2O concentration of 95% (v/v). Exchange procedures were carried out on ice to slow down the exchange process and exacerbate the H/D exchange differences. The isotopic exchange was successively quenched by adding formic acid (FA) to 0.6% (v/v) in a 1:1 ratio with the sample volume to a final pH 2.5. Samples were desalted in a Waters MassPREP™ Micro Desalting Columns (2.1 × 5 mm) cooled at 1°C. The elution was obtained by using a gradient of water containing FA (0.23% V/V) and acetonitrile containing FA (0.23% V/V) from 5% to 50% in 3 min, at a flow rate of 50 µl/min. Samples were analyzed by a Xevo G2-XS ESI-Q-TOF spectrometer (Waters Corporation, Milford, Massachusetts,

USA). A wash cycle was performed between each sample to avoid signal carry-over. The m/z spectra were deconvoluted by the software MaxEnt1. The level of back-exchange was calculated by using the following formula: $100\% - (Mass_{Fully\ deuterated} - Mass_{H2O})/(\#\ theoretical\ incorporation\ sites \times \%\ exchangeable\ D_2O\ in\ buffer)$.

4.9 | Statistical analysis

All data were reported as means values ± standard deviation (SD) of triplicates for HDX-MS analysis. The experiments were replicated eight times for SEC analysis and 12 times for ThT assay. Statistical analysis using one-way ANOVA, with p value < .05 as regarded statistically significant. The differences between control and experimental samples were determined by t-test.

AUTHOR CONTRIBUTIONS

Benedetta Fongaro: Conceptualization (equal); data curation (equal); formal analysis (equal); investigation (lead); validation (equal); visualization (lead). **Elia Cappelletto:** Data curation (equal); formal analysis (equal); investigation (equal); validation (supporting). **Alice Sosic:** Data curation (supporting); investigation (supporting); validation (supporting); writing – review and editing (supporting). **Barbara Spolaore:** Methodology (supporting); visualization (supporting). **Patrizia Polverino de Laureto:** Conceptualization (lead); data curation (lead); funding acquisition (lead); project administration (lead); resources (supporting); supervision (lead); writing – original draft (lead); writing – review and editing (lead).

ACKNOWLEDGMENTS

The authors thank Dr. Marino Bellini for the technical assistance in mass spectrometry and Federico Caicci for conducting TEM measurements. The authors are grateful to Dr. Luana Palazzi for fruitful discussion and to Ferdinando Polverino de Laureto for the graphical support. Open Access Funding provided by Universita degli Studi di Padova within the CRUI-CARE Agreement.

FUNDING INFORMATION

This research was supported by Progetti di Ateneo-University of Padova 2017 POLV_SID17 N. C93C1800002600, MIUR-PNRA to P.P. (Programma Nazionale Ricerche in Antartide) (grant number PNRA18_00147) and by Progetti di Ateneo-University of Padova 2018 SPOL_SID18_01. Preliminary data on this subject were presented at the Protein Society XXXV Annual Symposium, 7–14 July 2021, Comm. 48.

CONFLICTS OF INTEREST

The authors declare no conflict of interest. All authors have read and agreed to the published version of the manuscript.

ORCID

Patrizia de Polverino de Laureto https://orcid.org/0000-0002-0367-6781

REFERENCES

1. Kalia LV, Lang AE. Parkinson's disease. Lancet. 2015; 386(9996):896–912.
2. Spillantini MG, Murrell JR, Goedert M, Farlow MR, Klug A, Ghetti B. Mutation in the tau gene in familial multiple system tauopathy with presenile dementia. Proc Natl Acad Sci U S A. 1998;95(13):7737–7741.
3. Weinreb PH, Zhen W, Poon AW, Conway KA, Lansbury PT. NACP, a protein implicated in Alzheimer's disease and learning, is natively unfolded. Biochemistry. 1996;35(43):13709–13715.
4. Uversky VN. A protein-chameleon: Conformational plasticity of alpha-synuclein, a disordered protein involved in neurodegenerative disorders. J Biomol Struct Dyn. 2003;21(2):211–234.
5. Davidson WS, Jonas A, Clayton DF, George JM. Stabilization of alpha-synuclein secondary structure upon binding to synthetic membranes. J Biol Chem. 1998;273(16):9443–9449.
6. Eliezer D, Kutluay E, Bussell R, Browne G. Conformational properties of alpha-synuclein in its free and lipid-associated states. J Mol Biol. 2001;307(4):1061–1073.
7. Laureto PP, de Tosatto L, Frare E, Marin O, Uversky VN, Fontana A. Conformational properties of the SDS-bound state of alpha-synuclein probed by limited proteolysis: Unexpected rigidity of the acidic C-terminal tail. Biochemistry. 2006;45(38): 11523–11531.
8. Galvagnion C, Buell AK, Meisl G, et al. Lipid vesicles trigger α-synuclein aggregation by stimulating primary nucleation. Nat Chem Biol. 2015;11(3):229–234.
9. Ruzafa D, Hernandez-Gomez YS, Bisello G, Broersen K, Morel B, Conejero-Lara F. The influence of N-terminal acetylation on micelle-induced conformational changes and aggregation of α-synuclein. PLoS One. 2017;12(5):e0178576.
10. Luk KC, Kehm V, Carroll J, et al. Pathological α-synuclein transmission initiates Parkinson-like neurodegeneration in nontransgenic mice. Science. 2012;338(6109):949–953.
11. Qin L, Wu X, Block ML, et al. Systemic LPS causes chronic neuroinflammation and progressive neurodegeneration. Glia. 2007;55(5):453–462.
12. Hoyer W, Cherny D, Subramaniam V, Jovin TM. Impact of the acidic C-terminal region comprising amino acids 109-140 on alpha-synuclein aggregation in vitro. Biochemistry. 2004; 43(51):16233–16242.
13. Polymeropoulos MH, Lavedan C, Leroy E, et al. Mutation in the alpha-synuclein gene identified in families with Parkinson's disease. Science. 1997;276(5321):2045–2047.
14. Krüger R, Kuhn W, Müller T, et al. Ala30Pro mutation in the gene encoding alpha-synuclein in Parkinson's disease. Nat Genet. 1998;18(2):106–108.

15. Zarranz JJ, Alegre J, Gómez-Esteban JC, et al. The new mutation, E46K, of alpha-synuclein causes Parkinson and Lewy body dementia. Ann Neurol. 2004;55(2):164–173.
16. Proukakis C, Dudzik CG, Brier T, et al. A novel α-synuclein missense mutation in Parkinson disease. Neurology. 2013; 80(11):1062–1064.
17. Flagmeier P, Meisl G, Vendruscolo M, et al. Mutations associated with familial Parkinson's disease alter the initiation and amplification steps of α-synuclein aggregation. Proc Natl Acad Sci U S A. 2016;113(37):10328–10333.
18. Greenbaum EA, Graves CL, Mishizen-Eberz AJ, et al. The E46K mutation in alpha-synuclein increases amyloid fibril formation. J Biol Chem. 2005;280(9):7800–7807.
19. Burré J, Sharma M, Südhof TC. Systematic mutagenesis of α-synuclein reveals distinct sequence requirements for physiological and pathological activities. J Neurosci. 2012;32(43): 15227–15242.
20. Winner B, Jappelli R, Maji SK, et al. In vivo demonstration that alpha-synuclein oligomers are toxic. Proc Natl Acad Sci U S A. 2011;108(10):4194–4199.
21. Boyer DR, Li B, Sun C, et al. The α-synuclein hereditary mutation E46K unlocks a more stable, pathogenic fibril structure. Proc Natl Acad Sci U S A. 2020;117(7):3592–3602.
22. Rospigliosi CC, McClendon S, Schmid AW, et al. E46K Parkinson's-linked mutation enhances C-terminal-to-N-terminal contacts in alpha-synuclein. J Mol Biol. 2009;388(5): 1022–1032.
23. Fredenburg RA, Rospigliosi C, Meray RK, et al. The impact of the E46K mutation on the properties of alpha-synuclein in its monomeric and oligomeric states. Biochemistry. 2007;46(24): 7107–7118.
24. Wise-Scira O, Aloglu AK, Dunn A, Sakallioglu IT, Coskuner O. Structures and free energy landscapes of the wild-type and A30P mutant-type α-synuclein proteins with dynamics. ACS Chem Nerosci. 2013;4(3):486–497.
25. Zhao K, Li Y, Liu Z, et al. Parkinson's disease associated mutation E46K of α-synuclein triggers the formation of a distinct fibril structure. Nat Commun. 2020;11(1):2643.
26. Rovere M, Powers AE, Jiang H, et al. E46K-like α-synuclein mutants increase lipid interactions and disrupt membrane selectivity. J Biol Chem. 2019;294(25):9799–9812.
27. Fusco G, Pape T, Stephens AD, et al. Structural basis of synaptic vesicle assembly promoted by α-synuclein. Nat Commun. 2016;7:12563.
28. Bodner CR, Maltsev AS, Dobson CM, Bax A. Differential phospholipid binding of alpha-synuclein variants implicated in Parkinson's disease revealed by solution NMR spectroscopy. Biochemistry. 2010;49(5):862–871.
29. Meiser J, Weindl D, Hiller K. Complexity of dopamine metabolism. Cell Commun Signal. 2013;11(1):34.
30. Goldstein DS, Sullivan P, Holmes C, Lamotte G, Lenka A, Sharabi Y. Differential abnormalities of cerebrospinal fluid dopaminergic versus noradrenergic indices in synucleinopathies. J Neurochem. 2021;158(2):554–568.
31. Nunes C, Almeida L, Laranjinha J. 3,4-Dihydroxyphenylacetic acid (DOPAC) modulates the toxicity induced by nitric oxide in PC-12 cells via mitochondrial dysfunctioning. Neurotoxicology. 2008;29(6):998–1007.
32. Zhou W, Gallagher A, Hong D-P, Long C, Fink AL, Uversky VN. At low concentrations, 3,4-dihydroxyphenylacetic acid (DOPAC) binds non-covalently to alpha-synuclein and prevents its fibrillation. J Mol Biol. 2009;388(3):597–610.
33. Cicerale S, Lucas L, Keast R. Biological activities of phenolic compounds present in virgin olive oil. Int J Mol Sci. 2010;11(2): 458–479.
34. Yu G, Deng A, Tang W, Ma J, Yuan C, Ma J. Hydroxytyrosol induces phase II detoxifying enzyme expression and effectively protects dopaminergic cells against dopamine- and 6-hydroxydopamine induced cytotoxicity. Neurochem Int. 2016;96:113–120.
35. Palazzi L, Bruzzone E, Bisello G, et al. Oleuropein aglycone stabilizes the monomeric α-synuclein and favours the growth of non-toxic aggregates. Sci Rep. 2018;8(1):8337.
36. Palazzi L, Leri M, Cesaro S, Stefani M, Bucciantini M, Polverino de Laureto P. Insight into the molecular mechanism underlying the inhibition of α-synuclein aggregation by hydroxytyrosol. Biochem Pharmacol. 2020;173:113722.
37. Palazzi L, Fongaro B, Leri M, et al. Structural features and toxicity of α-Synuclein oligomers grown in the presence of DOPAC. Int J Mol Sci. 2021;22(11):6008.
38. Bousset L, Pieri L, Ruiz-Arlandis G, et al. Structural and functional characterization of two alpha-synuclein strains. Nat Commun. 2013;4:2575.
39. Dearborn AD, Wall JS, Cheng N, et al. α-Synuclein amyloid fibrils with two entwined, asymmetrically associated protofibrils. J Biol Chem. 2016;291(5):2310–2318.
40. Bertoncini CW, Jung Y-S, Fernandez CO, et al. Release of long-range tertiary interactions potentiates aggregation of natively unstructured alpha-synuclein. Proc Natl Acad Sci U S A. 2005; 102(5):1430–1435.
41. Stephens AD, Zacharopoulou M, Kaminski Schierle GS. The cellular environment affects monomeric α-synuclein structure. Trends Biochem Sci. 2019;44(5):453–466.
42. Trojanowski JQ, Lee VM-Y. Parkinson's disease and related alpha-synucleinopathies are brain amyloidoses. Ann N Y Acad Sci. 2003;991:107–110.
43. Íñigo-Marco I, Valencia M, Larrea L, et al. E46K α-synuclein pathological mutation causes cell-autonomous toxicity without altering protein turnover or aggregation. Proc Natl Acad Sci U S A. 2017;114(39):E8274–E8283.
44. Kumari P, Ghosh D, Vanas A, et al. Structural insights into α-synuclein monomer-fibril interactions. Proc Natl Acad Sci U S A. 2021;118(10):e2012171118.
45. Ranjan P, Kumar A. Perturbation in long-range contacts modulates the kinetics of amyloid formation in α-Synuclein familial mutants. ACS Chem Nerosci. 2017;8(10):2235–2246.
46. Grossi C, Rigacci S, Ambrosini S, et al. The polyphenol oleuropein aglycone protects TgCRND8 mice against Aß plaque pathology. PLoS One. 2013;8(8):e71702.
47. Leri M, Nosi D, Natalello A, et al. The polyphenol oleuropein aglycone hinders the growth of toxic transthyretin amyloid assemblies. J Nutr Biochem. 2016;30:153–166.
48. Tóth G, Neumann T, Berthet A, et al. Novel small molecules targeting the intrinsically disordered structural ensemble of α-synuclein protect against diverse α-Synuclein mediated dysfunctions. Sci Rep. 2019;9(1):16947.
49. Perni M, Galvagnion C, Maltsev A, et al. A natural product inhibits the initiation of α-synuclein aggregation and suppresses its toxicity. Proc Natl Acad Sci U S A. 2017;114(6): E1009–E1017.

50. Zafra-Gómez A, Luzón-Toro B, Capel-Cuevas S, Morales JC. Stability of hydroxytyrosol in aqueous solutions at different concentration, temperature and with different ionic content: A study using UPLC-MS. FNS. 2011;02(10):1114–1120.
51. De Francesch G, Frare E, Bubacco L, Mammi S, Fontana A, de Laureto PP. Molecular insights into the interaction between alpha-synuclein and docosahexaenoic acid. J Mol Biol. 2009; 394(1):94–107.
52. LeVine H. Quantification of β-sheet amyloid fibril structures with thioflavin T. Methods Enzymol. 1999;309:274–284.
53. Gill SC, von Hippel PH. Calculation of protein extinction coefficients from amino acid sequence data. Anal Biochem. 1989; 182(2):319–326.
54. Masson GR, Burke JE, Ahn NG, et al. Recommendations for performing, interpreting and reporting hydrogen deuterium exchange mass spectrometry (HDX-MS) experiments. Nat Methods. 2019;16(7):595–602.

SUPPORTING INFORMATION

Additional supporting information may be found in the online version of the article at the publisher's website.

How to cite this article: Fongaro B, Cappelletto E, Sosic A, Spolaore B, de Polverino de Laureto P. 3,4-Dihydroxyphenylethanol and 3,4-dihydroxyphenylacetic acid affect the aggregation process of E46K variant of α-synuclein at different extent: Insights into the interplay between protein dynamics and catechol effect. Protein Science. 2022;31(7):e4356. https://doi.org/10.1002/pro.4356